Using Machine Learning to Predict Core Sizes of High-Efficiency Turbofan Engines

Michael T. Tong
Glenn Research Center, Cleveland, Ohio

NASA STI Program . . . in Profile

Since its founding, NASA has been dedicated to the advancement of aeronautics and space science. The NASA Scientific and Technical Information (STI) Program plays a key part in helping NASA maintain this important role.

The NASA STI Program operates under the auspices of the Agency Chief Information Officer. It collects, organizes, provides for archiving, and disseminates NASA's STI. The NASA STI Program provides access to the NASA Technical Report Server—Registered (NTRS Reg) and NASA Technical Report Server—Public (NTRS) thus providing one of the largest collections of aeronautical and space science STI in the world. Results are published in both non-NASA channels and by NASA in the NASA STI Report Series, which includes the following report types:

- TECHNICAL PUBLICATION. Reports of completed research or a major significant phase of research that present the results of NASA programs and include extensive data or theoretical analysis. Includes compilations of significant scientific and technical data and information deemed to be of continuing reference value. NASA counter-part of peer-reviewed formal professional papers, but has less stringent limitations on manuscript length and extent of graphic presentations.

- TECHNICAL MEMORANDUM. Scientific and technical findings that are preliminary or of specialized interest, e.g., "quick-release" reports, working papers, and bibliographies that contain minimal annotation. Does not contain extensive analysis.

- CONTRACTOR REPORT. Scientific and technical findings by NASA-sponsored contractors and grantees.

- CONFERENCE PUBLICATION. Collected papers from scientific and technical conferences, symposia, seminars, or other meetings sponsored or co-sponsored by NASA.

- SPECIAL PUBLICATION. Scientific, technical, or historical information from NASA programs, projects, and missions, often concerned with subjects having substantial public interest.

- TECHNICAL TRANSLATION. English-language translations of foreign scientific and technical material pertinent to NASA's mission.

For more information about the NASA STI program, see the following:

- Access the NASA STI program home page at http://www.sti.nasa.gov

- E-mail your question to help@sti.nasa.gov

- Fax your question to the NASA STI Information Desk at 757-864-6500

- Telephone the NASA STI Information Desk at 757-864-9658

- Write to:
  NASA STI Program
  Mail Stop 148
  NASA Langley Research Center
  Hampton, VA 23681-2199

Using Machine Learning to Predict Core Sizes of High-Efficiency Turbofan Engines

Michael T. Tong
Glenn Research Center, Cleveland, Ohio

National Aeronautics and
Space Administration

Glenn Research Center
Cleveland, Ohio 44135

August 2019

Acknowledgments

The work presented in this paper was supported by the NASA Advanced Air Transport Technology Project of the Advanced Air Vehicles Program.

Level of Review: This material has been technically reviewed by technical management.

Available from

Using Machine Learning to Predict Core Sizes of High-Efficiency Turbofan Engines

Michael T. Tong
National Aeronautics and Space Administration
Glenn Research Center
Cleveland, Ohio 44135

Abstract

With the rise in big data and analytics, machine learning is transforming many industries. It is being increasingly employed to solve a wide range of complex problems, producing autonomous systems that support human decision-making. For the aircraft engine industry, machine learning of historical and existing engine data could provide insights that help drive for better engine design. This work explored the application of machine learning to engine preliminary design. Engine core-size prediction was chosen for the first study because of its relative simplicity in terms of number of input variables required (only three). Specifically, machine-learning predictive tools were developed for turbofan engine core-size prediction, using publicly available data of two hundred manufactured engines and engines that were studied previously in NASA aeronautics projects. The prediction results of these models show that, by bringing together big data, robust machine-learning algorithms and data science, a machine learning-based predictive model can be an effective tool for turbofan engine core-size prediction. The promising results of this first study paves the way for further exploration of the use of machine learning for aircraft engine preliminary design.

Introduction

In today's marketplace, rapid turnaround time of the investigation of new design concepts or technologies can be a powerful competitive advantage within the aircraft engine industry. To minimize risk, technological improvements of aircraft engine are generally made incrementally, drawing heavily from past experiences and lessons learned. Engine companies have generated and collected large amounts of data over the years. The big data, from various sources such as the database of currently manufactured engines and those of previously completed development projects, is a valuable resource of intelligence that can support new engine development. With increasing computational power, employing machine learning to mine these data can provide valuable insights and brings high levels of efficiency to engine preliminary design.

While the use of machine learning for aircraft engine preventive maintenance has been studied by a number of researchers (Refs. 1 and 2), its use for engine design has not been explored. In this work, supervised machine-learning algorithms were employed to find patterns in the database of two hundred manufactured engines and engines that were studied previously in various NASA aeronautics projects. Models (or analytics tools) to predict core sizes of axial-compressor turbofan engines that are being considered were built. The objective was to determine if machine learning-based predictive analytics could be an effective tool for turbofan engine core-size prediction. To be able to predict engine core size rapidly and accurately in the design space exploration would facilitate engine core architecture selection in the early stages of engine development. In this work, engine core size (h) is defined as:

$$h = \text{high-pressure compressor last-stage blade height}$$

The important aspect of this work was the extensive use of manufactured engine data (70 percent of the database). These engines span the era from the mid-1960s to mid-2010s. The database captures half-a-century of engine technology improvements and lessons-learned, which injects realism to the predictive models.

Turbofan Engine Core Size

The continuous drive for ever more efficient and quiet aircraft has resulted in the evolution of aircraft gas turbine engines from the earliest turbojet engines to today's turbofan engines with bypass ratios (BPR) of 6 to 12. The overall pressure ratio (OPR) of gas turbines has increased over time to improve thermodynamic efficiency. It is likely that the trend toward higher BPR and OPR engines will continue in the foreseeable future. Despite its benefits, the combination of increasing BPR and OPR will shrink the core size of high-pressure compressor (HPC), which can lead to rapid decrease of HPC efficiency due to increased sensitivity to tip clearance and airfoil manufacturing tolerances. A rule of thumb for the current-state-of-the-art engine design is that the HPC last-stage blade height should not be less than 0.5 in. (Ref. 3), to avoid this efficiency penalty. Figure 1 shows the efficiency penalty vs. HPC last-stage blade height of a NASA N+3 technology reference turbofan engine (Ref. 4).
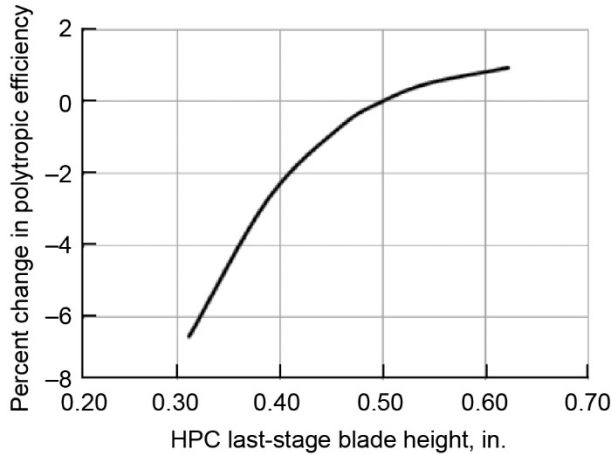
Figure 1.—HPC efficiency change vs. last-stage blade height of a NASA N+3 reference turbofan engine.

Machine Learning Algorithms

Machine learning is a branch of artificial intelligence that uses statistical technique and mathematical algorithms to enable a machine to learn from data, to analyze data patterns, and to make decisions with minimal human intervention. In this work, two machine-learning predictive models were developed for engine core-size classification, i.e., to label engine core size as *acceptable*, *unacceptable, etc.* Three different supervised machine-learning classification algorithms were used in these models. They are: k-nearest neighbors (KNN), support vector machines (SVM), and artificial neural network (ANN).

K-Nearest Neighbors (KNN) Classifier

KNN algorithm (Refs. 5 and 6) estimates how likely a data point belongs to a certain group based on what group its k nearest neighbors are in, where k is an integer value specified by the user. Each data point is weighted by the inverse of its Euclidean distance from its nearest neighbors. The optimal k is computed iteratively and the k value that give the lowest misclassification errors over the training dataset is selected. A grid-search routine was used to determine the optimal k value. KNN was implemented via the Python Scikit-Learn (Ref. 7) library class, *KNeighborsClassifier*.

Support Vector Machine (SVM) Classifier

A SVM (Refs. 5 and 8) classifier performs classification by finding an optimal hyperplane that maximizes the margin between the two classes. The hyperplane is a linear separator for any dimension. For nonlinearly-separated classes, a data transformation by a kernel function would be required. Kernel is a mathematical function that performs nonlinear transformation of data so that they can be classified by a linear hyperplane. In this work, a Gaussian (or radial basis function) kernel was used. It is a similarity function that measures the "distance" between a pair of data points and is defined as:

$$K\left(x,x'\right) = \exp\left(-\Upsilon\left\|x-x'\right\|^2\right)$$

where $\left\|x-x'\right\|$ is the Euclidean distance between two data points x and x'. And Υ (gamma) is a parameter that controls the tradeoff between error due to bias and variance in the model. Training SVM involves the minimization of the cost (or error) function (Refs. 3 and 6):

$$\frac{1}{2}\left\|w\right\|^2 + C\sum_{k=1}^{n}\xi_k$$

subject to the constraint:

$$y_k\left(w^T x_k + b\right) \geq 1 - \xi_k \text{ and } \xi_k \geq 0$$

where w = weight vectors
C = penalty parameter
ξ_k = slack parameters for handling non-separable data
T = transpose (of a matrix)
b = a constant
x_k = training data points
y_k = training data class labels

The penalty parameter C is a parameter in the cost function that controls the tradeoff between misclassification error and separation margin. Both Υ and the C have to be specified. A grid-search routine was used to determine the combination of Υ and C that gave the lowest misclassification error. SVM was implemented via the Python Scikit-Learn library class, *SVC*.

Artificial Neural Network (ANN) Classifier

ANN (Ref. 5), sometimes called multilayer perception, is a machine learning algorithm that attempts to mimic how the human brain processes information. An ANN is organized into input, hidden, and output layers. The hidden layer is composed of 'neurons', which process input variables and output the response variables, using activation functions. For this work, ANN consisted of one input layer, one hidden layer, and one output layer. A hyperbolic tangent (tanh) function was used for the activation functions in the hidden layer, defined as:

$$\tanh\left(x\right) = \frac{1-e^{-2x}}{1+e^{-2x}}$$

where x = weighted sum of input engine parameters

A grid-search routine was used to determine the regularization parameter (α) and the number of 'neurons' (N_e) in the hidden layer that gave the lowest misclassification error. ANN was implemented via the Python Scikit-Learn library class, *MLPClassifier.*

Engine Database

The basic engine architecture in this study was an axial-compressor turbofan. The engine database consisted of 139 manufactured engines (Refs. 9 to 15) and 61 engines that were studied previously in various NASA aeronautics projects. The NASA engine data were the system-study results for various NASA aeronautics projects (Refs. 16 to 22). The engine database is shown in the Appendix.

Predictive Models

Both 2-class and 3-class models were developed to predict engine core sizes in terms of classes, using the three machine learning algorithms described in the previous section. Core sizes of all the manufactured engines were assumed to be 0.5 in. or larger. For the NASA engines, core sizes were classified according to the blade-height data obtained from the system studies. Python programming language was used to develop both models.

Input engine parameters for both predictive models are:

- OPR at sea level static condition
- BPR at sea level static condition
- Sea level take-off thrust

The sea-level flight condition was chosen, to be consistent with the engine database (Appendix). The database was built based on publicly-available engine data.

The output is:

- Engine core size class label: *0, 1, or 2*

2-Class Predictive Model

This is a binary classification problem in machine learning. For this model, the engine core sizes were categorized into two classes: *0* and *1* (correspond to *acceptable* and *unacceptable* core sizes), according to the engine core size (h), as shown in Table 1.

TABLE 1.—CATEGORIES OF THE 2-CLASS MODEL

Two classes	
0 (acceptable)	*1* (unacceptable)
$h \geq 0.50$ in.	$h < 0.50$ in.

Training and building the predictive analytics involved machine-learning algorithms and data science. The approach consisted of three steps: dataset preparation; building, training, and cross-validation of the preliminary analytics; and building, training, and evaluation of the final analytics.

- Dataset preparation

The engine dataset was shuffled randomly (using pseudo-random number generator) and divided into two datasets: the training set and the testing set. The training set was used to train, cross-validate, and build predictive models. The testing set consisted of the remaining engines that were unseen by the predictive models, and was held out for the final evaluation of the predictive models. The training-testing dataset split is depicted in Table 2.

TABLE 2.—TRAINING-TESTING DATASET SPLIT FOR THE 2-CLASS MODEL

Core size	Training dataset, (number of engines)	Testing dataset (number of engines)
$h \geq 0.5$ in.	116	38
$h < 0.5$ in.	34	12
Total	150	50

- Preliminary training and cross-validation of the models

During preliminary training, three predictive 2-class models were developed using KNN, SVM, and ANN algorithms, respectively. This was done to identify the algorithm with the best accuracy for training a classifier to distinguish *acceptable* and *unacceptable* core sizes. The algorithm with the best performance was then selected to build and final-train the predictive model.

Within the training dataset (150 engines), a five-fold cross-validation procedure was used to conduct a preliminary evaluation and to fine-tune the models. The training dataset was randomly split into 5 groups: 4 groups were used to train the models and 1 group was used to cross-validate the models. This process was repeated 5 times so that each of the 5 groups got the chance to be used for training and validation. The performance measure was then the average of the values, in terms of the means and standard deviation, computed in the iteration loop.

- Building, training, and evaluation of the final model

The best algorithm is identified in the previous step was used to build and train the final predictive model. Cross-validation was no longer needed for this step, i.e., all 150 engine data were used to build and train the predictive model. The model was then used to predict the core sizes of the engines in the testing dataset (50 engines), and the results were compared with the testing dataset.

3-Class Predictive Model

In this model, the engine core sizes were categorized into three classes: *0, 1, and 2* (correspond to *acceptable, acceptable with improved manufacturing technologies*, and *unacceptable*, core sizes) according to the engine core size (*h*), as shown in Table 3. The training-testing dataset split is depicted in Table 4.

TABLE 3.—CATEGORIES OF THE 3-CLASS MODEL

Three classes		
0 (acceptable)	*1* (acceptable with improved manufacturing technologies)	*2* (unacceptable)
$h \geq 0.50$ in.	0.5 in. > h > 0.41 in.	$h \leq 0.41$ in.

TABLE 4.—TRAINING-TESTING DATASET SPLIT FOR THE 3-CLASS MODEL

Core size	Training dataset, (number of engines)	Testing dataset, (number of engines)
$h \geq 0.5$ in.	116	38
0.5 in. > h > 0.41 in.	17	6
$h \leq 0.41$ in.	17	6
Total	150	50

Similar to the 2-class model, the testing dataset consisted of the 50 engine that were unseen by the predictive models, and was held out for final evaluation of the predictive tools. Dataset preparation, model building, training, and evaluation procedures were similar to those for the 2-class model.

Predictive Results

2-Class Predictive Model

For this model, the training dataset consisted of 116 engines with $h \geq 0.5$ in. and 34 engines with $h < 0.5$ in. Using a grid-search routine, the parameters that gave the lowest misclassification errors for the three algorithms were determined. They are shown in Table 5.

TABLE 5.—ALGORITHMS USED AND THE PARAMETERS (2-CLASS MODEL)

Algorithms	Parameters
KNN	$k = 4$
SVM	$C = 10, \Upsilon = 2.0$
ANN	$\alpha = 0.001, N_e = 2.0$

The classification accuracy of the machine learning algorithms was defined as the number of correct predictions made as a percentage of all predictions made. And uncertainty was defined at 95 percent confidence interval, i.e., two standard deviations for normal data distribution. The preliminary training and cross-validation results are shown in Table 6.

TABLE 6.—CROSS-VALIDATION RESULTS (2-CLASS MODEL)

Algorithms	Accuracy, (mean), percent	Uncertainty 95% confidence interval, (2 standard deviations), percent
KNN	96	7
SVM	98	5
ANN	97	7

They show that SVM had the best accuracy and the lowest uncertainty. So, it was selected to build and final-train the predictive model.

The final predictive model, built with SVM algorithm, was then used to predict the engine core sizes in the testing dataset (the 50 engines unseen by the model). Performance metrics for final model evaluation are:

- Overall engine core-size prediction accuracy
- Unacceptable engine core-size ($h < 0.5$ in.) prediction accuracy

To be able to predict unacceptable engine core-size is the main objective of the predictive tool. The results are shown in Table 7.

TABLE 7.—FINAL TEST RESULTS OF THE 2-CLASS MODEL

Core size	Number of engines, (data)	Number of engines, (prediction)	Accuracy, percent
$h \geq 0.5$ in.	38	38	100
$h < 0.5$ in.	12	11	92
Overall	50	49	98

Overall, the 2-class model had an accuracy of 98 percent, with an uncertainty of 5 percent. More importantly, it predicted unacceptable engine core sizes with 92 percent accuracy. The results were compared with the testing dataset in Table 8. It shows only one engine was misclassified.

TABLE 8.—COMPARISON OF PREDICTED RESULTS WITH TESTING DATASET—TWO-CLASS MODEL

Org.	Engine model	Core size Data	Core size Prediction		Org.	Engine model	Core size Data	Core size Prediction
CFM Int'l	LEAP-1A35	●	●		NASA ERA	Large-DD-2014	●	●
NASA ERA	Small-DD-2015-V2	▲	▲		CFM Int'l	CFM56-7B22	●	●
NASA AATT	ND8-FPR1.5-DOE2	▲	▲		NASA ERA	Large-DD-2015-HWB-V2	●	●
Rolls Royce	BR715-C1-30	●	●		NASA ERA	Small-Geared-2014	▲	▲
NASA AATT	Small Core geared	▲	● ←		GE	GE90-85B	●	●
Rolls Royce	Trent XWB-97	●	●		Rolls Royce	BR715-A1-30	●	●
Rolls Royce	AE3007A	●	●		GE	GEnx-1B70/P2	●	●
GE	CF34-8C1	●	●		GE	CF6-80C2B1	●	●
Rolls Royce	Trent 1000-G3	●	●		NASA AATT	ND8-FPR1.6-DOE1	▲	▲
NASA SFW	SA-FPR1.4-DD-2D	▲	▲		CFM Int'l	CFM56-5B3	●	●
Rolls Royce	RB211-524C2	●	●		NASA ERA	Large-Geared-2015-HWB-V2	●	●
GE	CF34-8E5A2	●	●		NASA ERA	Medium-Geared-2015-V2	●	●
P&W	PW4462	●	●		P&W	PW2037	●	●
GE	Genx-1B58/P1	●	●		NASA AATT	TBW V2	▲	▲
NASA SFW	SA-FPR1.3-GR-HW-2D	▲	▲		CFM Int'l	CFM56-7B20	●	●
CFM Int'l	CFM56-2C1	●	●		P&W	PW4074	●	●
Rolls Royce	Trent XWB-84	●	●		P&W	PW1130G	●	●
Rolls Royce	RB211-524D4	●	●		CFM Int'l	CFM56-5A4	●	●
CFM Int'l	CFM56-5B5/P	●	●		GE	GE90-90B	●	●
NASA SFW	SA-FPR1.4-GR-HW-2D	▲	▲		CFM Int'l	CFM56-7B26	●	●
NASA ERA	Small-Geared-2015-V2	▲	▲		NASA AATT	ND8-FPR1.6-DOE2	▲	▲
Rolls Royce	Trent 875	●	●		IAE	IAE V2533-A5	●	●
Rolls Royce	Trent 1000-L3	●	●		GE	CF6-80A2	●	●
Rolls Royce	Trent 972-84	●	●		GE	CF6-80C2A1	●	●
NASA AATT	ND8 DOE2 FPR1.30	▲	▲		P&W	PW4084	●	●

● $h \geq 0.50$ in.   ▲ $h < 0.50$ in.   ← misclassification

3-Class Predictive Model

For this model, the training dataset consisted of 116 engines with $h \geq 0.5$ in., 17 engines with 0.5 in. $> h > 0.41$ in., and 17 engines with $h \leq 0.41$ in. Using a grid-search routine, the parameters that gave the lowest misclassification errors for the three algorithms were determined. They are shown in Table 9.

TABLE 9.—ALGORITHMS USED AND THE PARAMETERS (3-CLASS MODEL)

Algorithms	Parameters
KNN	$k = 4$
SVM	$C = 55$, $\Upsilon = 0.5$
ANN	$\alpha = 0.002$, $N_e = 4$

The classification accuracy of the three machine learning algorithms from the preliminary training and cross-validation of the predictive models are shown in Table 10.

TABLE 10.—CROSS-VALIDATION RESULTS (3-CLASS MODEL)

Algorithms	Accuracy, (mean), percent	Uncertainty 95% confidence interval, (2 standard deviations), percent
KNN	91	12
SVM	91	11
ANN	91	7

The cross-validation results show that the 3-class predictive models were less accurate than the 2-class model. This is because of insufficient core-size data to train the model.

The 3-class model is more complex and requires more data for training. The three algorithms show the same accuracy; however, the ANN algorithm had the lowest uncertainty. The final predictive model, built with ANN algorithm, was then used to predict the core sizes of the engines in the testing dataset (the 50 engines unseen by the model). By using the same metrics as that for the 2-class model, the overall results are summarized in Table 11.

Overall, the 3-class model using the ANN algorithm has an accuracy of 94 percent, with 7 percent uncertainty. Its prediction accuracy for engine core sizes $h < 0.5$ in. is 75 percent

TABLE 11.—FINAL TEST RESULTS OF THE 3-CLASS MODEL

Core size	Number of engines (data)	Number of engines (prediction)	Accuracy, percent
$h \geq 0.5$ in.	38	38	100
0.5 in. $> h > 0.41$ in.	6	5	83
$h \leq 0.41$ in.	6	4	67
Overall	50	47	94

(average of 83 and 67 percent). The results are compared with the testing dataset, in Table 12. It shows three engines were misclassified. Comparing to the 2-class predictive model, the 3-class predictive model is less accurate because of insufficient training data. As shown in Table 4, there were only 17 engines with 0.5 in. $> h > 0.41$ in. and 17 engines with $h \leq 0.41$ in. available for training.

Conclusions

Machine-learning predictive models were developed for turbofan engine core-size prediction, using the database of two hundred manufactured engines and engines that were studied previously in NASA aeronautics projects. The 2-class predictive model is very accurate; it has an overall accuracy of 98 percent, with 5 percent uncertainty. And it predicted unacceptable engine core sizes with 92 percent accuracy. The 3-class predictive model has an overall accuracy of 94 percent, with 7 percent uncertainty. Its prediction accuracy for engine core sizes $h < 0.5$ in. is 75 percent.

To further improve the accuracy (and reduce the uncertainty) of the 3-class predictive model, the database needs to be expanded. The 3-class model is more complex and requires more data for training. However, the limitation of publicly available engine data is a challenge to overcome. Overall, the results show that by bringing together sufficient (big) high quality data, robust machine-learning algorithms and data science, machine learning-based predictive model can be an effective tool for engine core-size prediction, which would facilitate engine core architecture selection in the early stages of engine development. The promising results of this first study paves the way for further exploration of the use of machine learning for aircraft engine preliminary design.

TABLE 12.—COMPARISON OF PREDICTED RESULTS WITH TESTING DATASET—THREE-CLASS MODEL

Org.	Engine model	Core size Data	Core size Prediction		Org.	Engine model	Core size Data	Core size Prediction
GE	CF6-80A2	●	●		GE	Genx-1B75/P2	●	●
NASA AATT	ND8-FPR1.3-DOE3	▲	■	←	P&W	PW4156	●	●
Rolls Royce	Trent 1000-CE3	●	●		Rolls Royce	Trent 875	●	●
GE	CF6-80E1A2	●	●		NASA AATT	STARC-ABL-2017	■	■
CFM Int'l	CFM56-5B6/P	●	●		NASA ERA	Small-Geared-2015-V2	■	■
NASA ERA	Small-DD-2015-V2	▲	▲		NASA SFW	SA-FPR1.4-DD-2D	▲	▲
Rolls Royce	AE3007A	●	●		Rolls Royce	Trent 1000-R3	●	●
GE	GEnx-1B70/P2	●	●		NASA AATT	ND8-FPR1.4-DOE3	■	■
NASA SFW	SA-FPR1.6-GR-HW-2E	■	●	←	CFM Int'l	CFM56-5B3	●	●
NASA SFW	SA-FPR1.6-GR-HW-2D	▲	■	←	Rolls Royce	Trent 877	●	●
NASA ERA	Large-Geared-2015-HWB	●	●		Rolls Royce	BR710-A1-10	●	●
GE	CF6-80E1A3	●	●		NASA ERA	Large-Geared-2015	●	●
GE	CF34-3A	●	●		CFM Int'l	CFM56-5C4	●	●
Rolls Royce	Trent XWB-84	●	●		NASA SFW	Simulated GE90-110B	●	●
NASA AATT	ND8-FPR1.5-DOE4	▲	▲		GE	Genx-1B54/P1	●	●
CFM Int'l	CFM56-5C2	●	●		GE	Genx-1B58/P1	●	●
NASA ERA	Large-DD-2014	●	●		CFM Int'l	LEAP-1A26	●	●
NASA AATT	ND8-FPR1.4-DOE1	■	■		Rolls Royce	Trent 1000-L3	●	●
CFM Int'l	CFM56-5A3	●	●		NASA AATT	ND8-FPR1.3-DOE1	■	■
Rolls Royce	Trent 1000-G3	●	●		CFM Int'l	CFM56-5C3	●	●
CFM Int'l	LEAP-1B25	●	●		NASA AATT	ND8-FPR1.6-DOE2	▲	▲
CFM Int'l	LEAP-1B27	●	●		CFM Int'l	CFM56-7B26	●	●
Rolls Royce	Trent 556-61	●	●		Rolls Royce	BR715-C1-30	●	●
NASA ERA	Large-Geared-2014	●	●		Rolls Royce	Trent 1000-H3	●	●
P&W	PW4168-1D	●	●		NASA SFW	Simulated Genx	●	●

● $h \geq 0.50$ in.   ■ 0.5 in. $> h > 0.41$ in.   ▲ $h \leq 0.41$ in.   ← misclassification

Appendix—Engine Database

Org.	Engine Model	OPR (SLS)	BPR (SLS)	Thrust, lbs (Take-off)	Core Size	Org.	Engine Model	OPR (SLS)	BPR (SLS)	Thrust, lbs (Take-off)	Core Size
GE	CF34-10A	26.5	5.4	18290	●	CFM Int'l	56-3B1	22.4	5.1	20000	●
GE	CF34-10E	27.3	5.09	18820	●	CFM Int'l	56-3B2	25.5	5.1	23500	●
GE	CF34-3A	19.7	6.25	9220	●	CFM Int'l	56-3C1	25.5	5.1	23500	●
GE	CF34-8C1	23.03	5.13	12670	●	CFM Int'l	56-5A1	26.6	6	25000	●
GE	CF34-8C5	23.09	5.13	13358	●	CFM Int'l	56-5A3	26.6	6	25000	●
GE	CF34-8E5A2	24.82	5.13	14500	●	CFM Int'l	56-5A4	23.8	6	22000	●
GE	CF6-80A	29	5	48000	●	CFM Int'l	56-5A5	25.1	6	23500	●
GE	CF6-80A2	30.1	5	50000	●	CFM Int'l	56-5B1	30.2	5.7	30000	●
GE	CF6-80C2A1	30.96	5.1	59000	●	CFM Int'l	56-5B2	31.3	5.6	31000	●
GE	CF6-80C2A5	31.58	5.1	60100	●	CFM Int'l	56-5B3	32.6	5.4	33300	●
GE	CF6-80C2A8	31	5.1	59000	●	CFM Int'l	56-5B4	27.1	5.9	26500	●
GE	CF6-80C2B1	30.08	5.1	56700	●	CFM Int'l	56-5B5/P	23.33	5.9	22000	●
GE	CF6-80C2B1F	30.13	5.1	57160	●	CFM Int'l	56-5B6/P	24.64	6	23500	●
GE	CF6-80C2B4	30.36	5.1	57180	●	CFM Int'l	56-5C2	28.8	6.8	31200	●
GE	CF6-80C2B6	31.56	5.1	60070	●	CFM Int'l	56-5C3	29.9	6.7	32500	●
GE	CF6-80E1A2	33.1	5.1	68240	●	CFM Int'l	56-5C4	31.15	6.6	34000	●
GE	CF6-80E1A3	35.7	5.1	68520	●	CFM Int'l	56-7B20	22.61	5.4	20600	●
GE	CF6-80E1A4	34.5	5.1	66870	●	CFM Int'l	56-7B22	24.41	5.3	22700	●
GE	90-115B	42.24	7.08	115500	●	CFM Int'l	56-7B24	25.78	5.2	24200	●
GE	90-76B	35.45	8.6	79654	●	CFM Int'l	56-7B26	27.61	5.1	26400	●
GE	90-85B	38.37	8.44	87315	●	CFM Int'l	56-7B27	28.63	5	28900	●
GE	90-90B	39.7	8.4	94000	●	CFM Int'l	LEAP-1A26	33.4	11.1	27112	●
GE	90-94B	40.82	8.33	96870	●	CFM Int'l	LEAP-1A35	38.6	10.7	32170	●
GE	Genx-1B54/P1	35.1	9.4	57400	●	CFM Int'l	LEAP-1B25	38.4	8.4	26797	●
GE	Genx-1B58/P1	37.1	9.2	60991	●	CFM Int'l	LEAP-1B27	39.9	8.5	28034	●
GE	Genx-1B64/P1	40.5	9	66993	●	CFM Int'l	LEAP-1B28	41.5	8.6	29315	●
GE	Genx-1B67/P1	41.9	8.9	69399	●	Engine Alliance	GP7270	36.62	8.71	74724	●
GE	GEnx-1B70/P2	43.9	8.8	72300	●	IAE	V2500-A1	29.8	5.3	25000	●
GE	GEnx-1B74/75	46.4	8.7	76705	●	IAE	V2522-A5	25.7	4.9	23043	●
GE	Genx-1B75/P2	47	8.6	77604	●	IAE	V2524-A5	26.9	4.81	24518	●
GE	GEnx-1B76/P2	47.5	8.6	78503	●	IAE	V2525-D5	27.2	4.82	25000	●
GE	Genx-2B67	43.6	8	67400	●	IAE	V2527-A5	27.2	4.82	25000	●
CFM Int'l	56-2C1	23.5	6	22000	●	IAE	V2528-D5	30	4.66	28000	●

● $h \geq 0.50$ in.   ■ 0.5 in. $> h > 0.41$ in.   ▲ $h \leq 0.41$ in.

Org.	Engine Model	OPR (SLS)	BPR (SLS)	Thrust, lbs (Take-off)	Core Size	Org.	Engine Model	OPR (SLS)	BPR (SLS)	Thrust, lbs (Take-off)	Core Size
IAE	V2530-A5	32	4.6	29900	●	P&W	1525G	38.7	11.1	24392	●
IAE	V2533-A5	33.44	4.46	31600	●	Rolls-Royce	RB211-22B-02	24.7	4.7	42000	●
P&W	JT9D-20	20.3	5.2	46300	●	Rolls-Royce	RB211-524B-02	29	4.4	50000	●
P&W	JT9D-59A	24.5	4.9	53000	●	Rolls-Royce	RB211-524C2	29.1	4.5	50500	●
P&W	JT9D-7	22.2	5.15	46300	●	Rolls-Royce	RB211-524D4	29.7	4.3	52000	●
P&W	JT9D-7A	20.3	5.1	46950	●	Rolls-Royce	RB211-524G	32.1	4.25	56900	●
P&W	JT9D-7F	22.8	5.1	48000	●	Rolls-Royce	RB211-524H	34	4.2	59400	●
P&W	JT9D-7J	23.5	5.1	50000	●	Rolls-Royce	RB211-535C	21.5	4.5	36700	●
P&W	JT9D-7Q	24.5	4.9	53000	●	Rolls-Royce	RB211-535E4	25.4	4.1	39600	●
P&W	JT9D-7R4E	24.2	5	50000	●	Rolls-Royce	Trent 1000-A	9.47	41	70000	●
P&W	JT9D-7R4G2	26.3	4.8	54750	●	Rolls-Royce	Trent 1000-AE3	9	43	69893	●
P&W	2037	26.9	6.04	37600	●	Rolls-Royce	Trent 1000-CE3	9	45.8	75244	●
P&W	2040	29.4	5.54	40900	●	Rolls-Royce	Trent 1000-G3	9.1	44.5	72771	●
P&W	4052	26.32	5	52200	●	Rolls-Royce	Trent 1000-H3	9.3	40.1	64543	●
P&W	4056	29.3	4.7	56750	●	Rolls-Royce	Trent1000-J3	47.8	8.9	78885	●
P&W	4060	32.4	4.5	60000	●	Rolls-Royce	Trent 1000-L3	45.8	9	75244	●
P&W	4074	32.2	6.8	74500	●	Rolls-Royce	Trent 1000-M3	48.7	8.9	80504	●
P&W	4077	33.2	6.7	77000	●	Rolls-Royce	Trent 1000-P3	45.8	9	75244	●
P&W	4084	36.2	6.4	84000	●	Rolls-Royce	Trent 1000-R3	49.4	8.9	81810	●
P&W	4090	39.16	6.1	90200	●	Rolls-Royce	Trent 553-61	35.19	7.5	56620	●
P&W	4098	41.37	5.8	95340	●	Rolls-Royce	Trent 556-61	36.7	7.5	56620	●
P&W	4152	26.9	4.9	52200	●	Rolls-Royce	Trent 7000-72	45.4	9	73700	●
P&W	4156	29.3	4.7	56750	●	Rolls-Royce	Trent 768	34	5.15	68400	●
P&W	4164	31.24	5.2	64000	●	Rolls-Royce	Trent 772	35.8	5.03	71000	●
P&W	4168-1D	33.1	4.92	68600	●	Rolls-Royce	Trent 875	35.42	6.08	79100	●
P&W	4460	30.68	4.7	60000	●	Rolls-Royce	Trent 877	36.3	6.02	81300	●
P&W	4462	31.91	4.6	63300	●	Rolls-Royce	Trent 884-17	38.96	5.95	87700	●
P&W	1122G	28.8	12.7	24234	●	Rolls-Royce	Trent 892-17	41.38	5.7	92500	●
P&W	1127G	31.7	12.3	27000	●	Rolls-Royce	Trent 895	41.52	5.7	92900	●
P&W	1129G	34	12	29248	●	Rolls-Royce	Trent 970-84	38	8.5	76143	●
P&W	1130G	38.1	11.6	33114	●	Rolls-Royce	Trent 970B-84	39.4	8.4	79335	●
P&W	1519G	32.3	11.6	19800	●	Rolls-Royce	Trent 972-84	38.7	8.4	77761	●
P&W	1521G	35.1	11.4	21964	●	Rolls-Royce	Trent XWB-75	36.8	9.3	75086	●

● $h \geq 0.50$ in.   ■ 0.5 in. > h > 0.41 in.   ▲ $h \leq 0.41$ in.

Org.	Engine Model	OPR (SLS)	BPR (SLS)	Thrust, lbs (Take-off)	Core Size	Org.	Engine Model	OPR (SLS)	BPR (SLS)	Thrust, lbs (Take-off)	Core Size
Rolls-Royce	Trent XWB-79	38.8	9.2	79852	●	NASA ERA	Medium-Geared-2015	38.4	23.9	45829	●
Rolls-Royce	Trent XWB-84	41.1	9	85200	●	NASA ERA	Medium-Geared-2015-V2	38.5	24.8	45799	●
Rolls-Royce	Trent XWB-97	48.6	8	98200	●	NASA ERA	Small-DD-2014	29.7	9.8	15566	▲
Rolls-Royce	BR710-A	24.23	4.2	14750	●	NASA ERA	Small-DD-2015	28.7	9.9	14647	▲
Rolls-Royce	BR715-A	28.98	4.66	18920	●	NASA ERA	Small-DD-2015-V2	28.7	10	14686	▲
Rolls-Royce	BR715-C	32.15	4.55	21430	●	NASA ERA	Small-Geared-2014	29.2	24.7	24887	■
Rolls Royce	AE3007A	18.08	5.23	7580	●	NASA ERA	Small-Geared-2015	24.6	27	21525	■
NASA SFW	50-pax	37.2	11.2	5925	▲	NASA ERA	Small-Geared-2015-V2	24.8	27.4	21553	■
NASA SFW	Simulated Genx	41.4	9.2	63800	●	NASA AATT	N3CC-2016	31.6	17.6	18830	■
NASA SFW	Simulated GE90-110B	42	7.2	110000	●	NASA AATT	N3CC-2017	36.9	17.3	21515	■
NASA SFW	UHB	44.7	18.8	36833	●	NASA AATT	N3CC-2018	36.7	21.6	21662	▲
NASA SFW	SA-FPR1.3-GR-HW-2E	32.3	26	28358	■	NASA AATT	STABL-2017	18	15.7	12139	■
NASA SFW	SA-FPR1.4-GR-HW-2E	33.8	18	26575	■	NASA AATT	STARC-ABL-2017	34.7	12.8	21954	■
NASA SFW	SA-FPR1.5-GR-HW-2E	35.4	12.1	24686	■	NASA AATT	STARC-ABL-2018	33.9	15	16872	▲
NASA SFW	SA-FPR1.6-GR-HW-2E	36.3	9.9	24262	■	NASA AATT	ND8-FPR1.3-DOE1	28.5	29.2	25633	■
NASA SFW	SA-FPR1.7-DD-LW-2E	37.6	8.5	23889	●	NASA AATT	ND8-FPR1.3-DOE2	26.4	33.3	25633	■
NASA SFW	SA-FPR1.4-DD-2D	33.1	18.4	23813	▲	NASA AATT	ND8-FPR1.3-DOE3	32.5	28.9	28196	▲
NASA SFW	SA-FPR1.5-DD-2D	33.8	15	23370	▲	NASA AATT	ND8-FPR1.4-DOE1	29.8	25.9	25633	■
NASA SFW	SA-FPR1.6-DD-2D	34.4	12.7	23046	■	NASA AATT	ND8-FPR1.4-DOE2	34.8	19.8	25633	■
NASA SFW	SA-FPR1.7-DD-2D	35	10.9	22734	■	NASA AATT	ND8-FPR1.4-DOE3	31.9	23	25633	■
NASA SFW	SA-FPR1.3-GR-HW-2D	32.6	24.1	26343	▲	NASA AATT	ND8-FPR1.4-DOE4	40.2	19.4	28196	▲
NASA SFW	SA-FPR1.4-GR-HW-2D	33.8	17.5	24917	▲	NASA AATT	ND8-FPR1.5-DOE1	37.5	17	25633	▲
NASA SFW	SA-FPR1.5-GR-HW-2D	33.5	14.6	23369	▲	NASA AATT	ND8-FPR1.5-DOE2	34.8	19.4	25633	■
NASA SFW	SA-FPR1.6-GR-HW-2D	34	12.4	22924	▲	NASA AATT	ND8-FPR1.5-DOE3	29.6	20.2	23070	■
NASA ERA	Large-DD-2014	47.4	16.2	80071	●	NASA AATT	ND8-FPR1.5-DOE4	48.6	13.9	28196	▲
NASA ERA	Large-DD-2015	43.7	16.6	71792	●	NASA AATT	ND8-FPR1.6-DOE1	33.6	15.9	23070	▲
NASA ERA	Large-DD-2015-HWB-V1	49.8	13.7	67183	●	NASA AATT	ND8-FPR1.6-DOE2	43.2	13.2	25633	▲
NASA ERA	Large-DD-2015-HWB-V2	48.9	14.4	67233	●	NASA AATT	ND8-FPR1.6-DOE3	39.8	15.1	25633	▲
NASA ERA	Large-Geared-2014	47.2	22.4	87496	●	NASA AATT	N+3	27.5	36.6	28620	■
NASA ERA	Large-Geared-2015	39.9	24.7	74149	●	NASA AATT	Small Core geared	38.8	25.5	37659	■
NASA ERA	Large-Geared-2015-HWB	47.2	19.3	67386	●	NASA AATT	TBW-MDP	23.6	0.41	17416	▲
NASA ERA	Large-Geared-2015-HWB-V2	47.1	20	67423	●	NASA AATT	TBW-hFan	17.3	0.31	28347	▲
NASA ERA	Large-Geared-2015-HWB-V3	47.2	20	56172	■	NASA AATT	TBW-V2	19.2	0.36	23049	▲
NASA ERA	Medium-Geared-2014	44.7	22.4	51295	●	NASA AATT	TBW-V3	20.3	0.34	22242	▲

SFW – NASA Subsonic Fixed Wing project   ERA – NASA Environmentally Responsible Aviation project   AATT – NASA Advanced Air Transport Technology project

● $h \geq 0.50$ in.   ■ 0.5 in. $> h > 0.41$ in.   ▲ $h \leq 0.41$ in.

References

1. Microsoft Azure Machine Learning Team, "Predictive Maintenance for Aircraft Engines." https://blog.revolutionanalytics.com/2016/05/predictive-maintenance-r-code.html

2. RT Insights Team, "How Rolls-Royce Maintains Jet Engines With the IoT." October 11, 2016. https://www.rtinsights.com/rolls-royce-jet-engine-maintenance-iot/

3. Larsson, L., Gronstedt, T., Kyprianidis, K.G., "Conceptual Design and Mission Analysis for a Geared Turbofan and an Open Rotor Configuration," GT2011-46451. Proceedings of ASME Turbo Expo 2011, June 6-10, 2011.

4. Jones, S.M., Haller, W.J., Tong, M.T., "An N+3 Technology Level Reference Propulsion System," NASA TM- 2017-219501, May, 2017.

5. Ng, A., "Machine Learning," Coursera online course lecture notes. https://www.coursera.org/learn/machine-learning

6. "Nearest Neighbor Classifier," CS231 lecture notes. Stanford University. http://cs231n.github.io/classification/#nn

7. Pedregosa *et al.*, "Scikit-learn: Machine Learning in Python," The Journal of Machine Learning Research, 12, pp. 2825-2830, 2011.

8. Ng, A., "Support Vector Machines." CS229 lecture notes. Stanford University. http://cs229.stanford.edu/notes/cs229-notes3.pdf

9. Daly, M., "Jane's Aero-Engine," 2017-2018.

10. Meier, N., "Civil turbojet/turbofan specifications." http://www.jet-engine.net/civtfspec.html. Accessed August, 2018.

11. GE Aviation. https://www.geaviation.com/commercial

12. Pratt and Whitney. https://www.pw.utc.com/products-and-services/products/commercial-engines

13. Rolls Royce. https://www.rolls-royce.com/products-and-services/civil-aerospace

14. CFM International. https://www.cfmaeroengines.com/

15. International Civil Aviation Organization, "ICAO Aircraft Emissions Databank." May, 2018.

16. Guynn, M.D., Berton, J.J., Fisher, K.L., Haller, W.J., Tong, M., Thurman, D.R., "Engine Conceptual Study for an Advanced Single-Aisle Transport," NASA TM-2009-215784, August 2009.

17. Guynn, M.D., Berton, J.J., Fisher, K.L., Haller, W.J., Tong, M., Thurman, D.R., "Analysis of Turbofan Design Options for an Advanced Single-Aisle Transport Aircraft," AIAA 2009-6942, September 2009.

18. Guynn, M. D., Berton, J.J., Fisher, K.L., Haller, W.J., Tong, M., Thurman, D.R, "Refined Exploration of Turbofan Design Options for an Advanced Single-Aisle Transport," NASA TM-2011-216883, January 2011.

19. Guynn, M.D., Berton, J.J., Tong, M.T., Haller, W.J., "Advanced Single-Aisle Transport Propulsion Design Options Revisited," AIAA 2013-4330, August 2013.

20. Nickol, C.L. and Haller W.J., "Assessment of the Performance Potential of Advanced Subsonic Transport Concepts for NASA's Environmentally Responsible Aviation Project," AIAA 2016-1030, January 2016.

21. Collier, F., Thomas, R., Burley, C., Nickol, C., Lee, C.M., Tong, M., "Environmentally Responsible Aviation - Real Solutions for Environmental Challenges Facing Aviation," 27th International Congress of the Aeronautical Sciences, September, 2010.

22. Welstead, J.R., Felder J.L., "Conceptual Design of a Single-Aisle Turboelectric Commercial Transport with Fuselage Boundary Layer Ingestion." AIAA 2016-1027, January 2016.